HHS Public Access

Author manuscript

Pain. Author manuscript; available in PMC 2018 March 01.

Published in final edited form as:

Pain. 2017 March ; 158(3): 488–497. doi:10.1097/j.pain.0000000000000788.

Brain activity for tactile allodynia: a longitudinal awake rat fMRI study tracking emergence of neuropathic pain

Pei-Ching Chang[1], **Maria Virginia Centeno**[1], **Daniel Procissi**[2], **Alex Baria**[1], and **A. Vania Apkarian**[1,*]

[1]Department of Physiology, Northwestern University Feinberg School of Medicine, Chicago, Illinois 60611, USA

[2]Department of Radiology, Northwestern University Feinberg School of Medicine, Chicago, Illinois 60611, USA

Abstract

Tactile allodynia, a condition in which innocuous mechanical stimuli are perceived as painful, is a common feature of chronic pain. However, how the brain reorganizes in relation to the emergence of tactile allodynia is still largely unknown. This may stem from the fact that experiments in humans are cross-sectional in nature, while animal brain imaging studies typically require anaesthesia rendering the brain incapable of consciously sensing or responding to pain. In this longitudinal fMRI study in awake rats, we tracked brain activity with the development of tactile allodynia. Prior to injury, innocuous air puff stimuli evoked a distributed sensory network of activations, including contralateral somatosensory cortices, thalamus, insula, and cingulate cortex. Moreover, the primary somatosensory cortex displayed a graded response tracking airpuff stimulus intensities. After neuropathic injury, and for stimuli where the intensity exceeded the paw withdrawal threshold (evoking tactile allodynia), the BOLD response in the primary somatosensory cortex was equivalent to that evoked by the identical stimulus prior to injury. In contrast, nucleus accumbens and prefrontal brain areas displayed abnormal activity to normally innocuous stimuli when such stimuli induced tactile allodynia at 28 days after peripheral nerve injury, which had not been the case at 5 days post-injury. Our data indicate that tactile allodynia-related nociceptive inputs are not observable in the primary somatosensory cortex BOLD response. Instead, our data suggests that, in time, tactile allodynia differentially engages neural circuits that regulate the affective and motivational components of pain.

Introduction

Tactile allodynia, pain arising from normally innocuous stimuli, is a common feature of neuropathic pain [24; 49]. Patients with tactile allodynia can experience severe pain sensations from the mild pressure of clothing, a light touch, or even a breeze on the affected area. The majority of research into tactile allodynia has concentrated on changes in the peripheral nervous system and spinal cord circuitry [10; 13; 19; 42]. The resultant general

*Correspondence should be addressed to: Dr. A. Vania Apkarian (a-apkarian@northwestern.edu). Address: Northwestern University, 303 East Chicago Avenue, Tarry Bldg. 7-705, Chicago, Illinois 60611, USA.

Conflict of Interest: The authors declare no competing financial interests.

hypothesis is that it is a consequence of nerve injury causing changes in tactile signaling in the spinal cord. That is, following central sensitization, low-threshold Aβ fibers normally mediating tactile sensation gain access to the nociceptive system in the spinal cord. As a result, innocuous tactile stimuli activating Aβ fibers evoke painful sensations.

Although it is widely recognized that the involvement of supraspinal loops cannot be excluded in tactile allodynia, to date we still have a limited knowledge of the role of related cortical and subcortical mechanisms. The standard general hypothesis implies that, following an allodynia causing injury, mechanical innocuous stimuli should engage and enhance the brain circuitry commonly observed for acute pain. The concept has been tested in brain imaging studies in healthy subjects following a mild skin injury [33], and in various neuropathic chronic pain patient groups exhibiting tactile allodynia [12; 21; 23; 30; 39]. Unfortunately, these studies do not present a coherent view of underlying circuitry, perhaps due to the diverse types of chronic pain studied and the cross-sectional designs employed. In this study, we take advantage of rodent models of neuropathic pain, since the emergence of neuropathic pain can be followed both before and at various time points after a neuropathic injury.

In this longitudinal study, we examine fMRI brain activity underlying touch-evoked allodynia in rats with neuropathic pain. Our primary goal is to understand how the brain representation for innocuous stimuli changes in relation to tactile allodynia in a homogeneous group of rats in comparison to sham injury, and as a function of time from peripheral neuropathic injury. To our knowledge, this is the first longitudinal fMRI study in awake rats. The use of awake rats enables us to examine how the brain consciously processes tactile allodynia for a range of innocuous stimuli which may not be detectable in fMRI studies in anesthetized rats [38; 40].

Methods

Animals

Twenty-two adult male Sprague Dawley rats (Harlan, Indianapolis, IN; 325g) were used in the present study. Rodents were housed on soft bedding in groups of two or three per cage on a 12-hour light/dark cycle in a temperature controlled environment (21 ± 2°C) with food and water available *ad libitum*. All animal handling and testing was performed during the light period. All of the experimental procedures were approved by Institutional Animal Care and Use Committee of Northwestern University.

Head-Post Implantation

Surgery for head-post implantation was done under anesthesia. Rats were initially anesthetized with 3.5% isoflurane mixed with 30% N_2 and 70% O_2, then transferred to a stereotaxic device and mounted using blunt ear bars that do not break the eardrums. Anesthesia was continued at a lower concentration sufficient to block motor responses to pinching the hindlimbs. The head fur was shaved, and eyes were covered with ointment to prevent drying out and corneal infection. After disinfecting the skin overlying the skull, the scalp was cut longitudinally and the skin retracted from the cranium. The head-post was

placed at the midpoint of bregma and lambda, and fixed to the skull with dental cement. The skin wound was treated with antibiotics. The animals were then released from the stereotaxic frame and kept warm using a heat lamp. After head-post implantation, rats were given at least a week of rest to recover from the surgical preparation prior to the start of acclimation procedures.

Spared Nerve Injury (SNI)

SNI was used as an animal model of peripheral neuropathic pain. Animals were anesthetized with isoflurane (1.5–2%) and a mixture of 30% N_2 and 70% O_2. The sciatic nerve of the left hind leg was exposed at the level of trifurcation into the sural, tibial, and common peroneal nerves. The tibial and common peroneal nerves were tightly ligated and severed, leaving the sural nerve intact. Sham animals had their sciatic nerves exposed as in the SNI procedure but received no further manipulations.

Test for Tacile Allodynia

Tactile sensitivty was assessed by withdrawal responses to von Frey filaments. The test was always performed one day before scanning, in a blinded paradigm. Rats whose head-posts became detached were excluded. The tactile sensitivity of the hind paw was measured using withdrawal responses to a series of von Frey filaments [17]. Rats were placed in a Plexiglass box with a wire grid floor and allowed to habituate to the environment for 10 – 15 minutes prior to testing. Filaments of varying forces (Stoelting Co, USA) were applied to the lateral part of the plantar surface of the hind paw. Filaments were applied in either ascending or descending strengths to determine the filament strength closest to the hind paw withdrawal threshold. Each filament was applied for a maximum of 2 seconds, with 10 seconds between each application. Testing continued until at least 6 measurements were completed after the first change in direction. Paw withdrawal during the stimulation was considered a positive response. Given the response pattern and the force of the final filament, 50% response threshold (in grams) was calculated.

Acclimation Procedure

Rats were habituated to the head-fix system using a short and systematic graded training procedure [16]. The acclimation included 1) body restraint with rats entering a snuggle sack by themselves and assuming a comfortable, natural posture, 2) immobilization of their head with a head-post, 3) air-puff stimulation to their paw, and 4) exposure to loud noise from fMRI scan sequences. Procedures for acclimation were carried out 30 minutes per day for 8–10 days during the 2 weeks prior to collection of imaging data. The procedures were repeated for 1–3 days prior to imaging at 5 and 28 days post surgery.

fMRI Experiments

The experimental design is illustrated in Figure 1. A total of 22 rats were used in the experiment. Baseline fMRI scans were conducted in rats 2 days prior to SNI (N = 12) or sham injury (N = 10). At 5 and 28 days post-injury, SNI and sham injury rats were scanned again. Animals whose head-post became detached during re-training sessions were not imaged. In addition, data from rats with excessive motion artifacts were likewise discarded.

After these eliminations, we retained scans for 10 SNI and 9 sham rats at day 5, and 7 SNI and 6 sham rats at day 28. The fMRI scans had 6 repetitive stimulus blocks for 5 minutes. Each block consisted of stimulation alternated with 8sec-off/12sec-on/30sec-off. FMRI scans during blocks of stimulation were acquired when the rats were awake and received unilateral 1g or 3g air-puff stimuli to the side surface of their hind paw via the outlet of the custom-made air-puff injector. Air-puffs were given continuously during the 12-second stimulation period. The force of air-puff is measured based on the weight it exerts on a balance scale. The 4^{th} fMRI scan, in which 3g stimuli was applied to the surgery paw, was intended to evoke tactile allodynia in the SNI rats after surgery.

To assess the behavioral response caused by the air-puff stimulation in the SNI animals, we performed a pilot test in which response to 3g air-puff stimulation was measured in a separate group of SNI rats at 45 days post-surgery (N = 2). The setup was identical to the real fMRI experiment except it was performed outside of the scanner. SNI rats exhibited minor paw movements and signs of motor weakness during stimulation to the injured paw, but no vocalization or other signs of distress or pain was observed. No response was seen when the stimulation was applied to the healthy paw.

During all fMRI experiments, respiratory rates were monitored using respiration pads (Model 1025; SA Instruments, Stony Brook, NY, USA). Respiratory waves were recorded during image acquisition with a sample rate of 225 samples per second.

MRI Acquisition

All MR experiments were carried out on a Bruker 7 T Clinscan horizontal magnet. A two-channel volume resonator was used for radio-frequency transmission and a 2 cm diameter surface coil was used for signal detection. Blood Oxygenation Level Dependent (BOLD) contrast-sensitive T2*-weighted EPI were acquired for functional images with the following parameters: gradient-echo, 16 oblique transverse slices, repetition time (TR) = 2000 ms, echo time (TE) = 18 ms, in-plane resolution = 0.38 mm × 0.38 mm, slice thickness = 0.5 mm, number of repetition is 150.

A T2-weighted anatomical image, with an identical spatial dimension to the functional images, was used as a main anatomical reference. An additional T2-weighted anatomical image with full-brain coverage was also obtained. Furthermore, field maps with short TE = 4 ms and long TE = 5 ms were collected.

Image Preprocessing

Images were preprocessed with FSL 5.1. All images were first skull stripped to remove non-brain voxels. Functional images were corrected for image distortion from the field map and imaging parameters. The functional images were then preprocessed with correction of slice-timing, motions, spatially smoothed with a Gaussian kernel of 0.7 mm full width at half maximum (FWHM) and high pass filtered with a cutoff of 100 seconds.

For each scan, each functional image was first aligned to the average of all functional images within the scan as reference image, and then registered to the main anatomical reference using a boundary-based registration (BBR) cost function. This was followed by an alignment

with the individual's full-brain anatomical image, and then co-registered to a full-brain standard space.

The time points in an fMRI dataset that were corrupted by large motion were detected using FSL's motion outliers routine. Outlier points were those that fell outside 1.5 times the interquartile range (0.25–0.75 quartile). Voxel-wise regressors for physiological noise, which was based on respiratory recording, were generated using the FSL tool PNM. Nuisance regressors that modeled six motion parameters (translations and rotations), motion spikes, and physiological noise were removed from fMRI data through linear regression.

Statistical Analysis

A general linear model (GLM) approach was performed on individual rodents to identify brain regions in which the time course of the BOLD signal was significantly related to the stimulation paradigm. After preprocessing, time series statistical analysis was carried out with FILM with local autocorrelation correction. The GLM model was convolved with a gamma hemodynamic response function with 0 second phase, 2 second FMWH, and 2.5 second lag to peak along its temporal derivative [46].

Group-level mixed effects group analyses were performed for each contrast by using FSL's FLAME module with two stages (1+2). The signal change of time points in a voxel was expressed as percentage changes relative to 8 seconds prior to the stimulus. A co-registered digital rat atlas [44] was used to label brain areas of interest.

Results

Behavioral Signs of Tactile Allodynia

Withdrawal thresholds of the injured paw in SNI animals, but not sham animals, decreased at 5 days post surgery (4.5 ± 0.58, mean ± SEM) and persisted at 28 days post surgery (2.65 ± 0.35) (Figure 1B; ANOVA, group by time effect $F(2, 57) = 8.75$, $p < 0.001$). Post-hoc testing revealed that the thresholds of SNI compared to sham rats did not differ at baseline, but were significantly different at both 5 and 28 days post SNI (Fisher LSD post-hoc comparison, $p < 0.001$). No changes in withdrawal thresholds were observed for the healthy paw in SNI or sham animals (Figure 1B, $F(2, 57) = 0.20$, $p = 0.82$).

Brain Representation of Tactile Stimulation in Healthy Rats

To characterize the brain responses to innocuous tactile stimuli in healthy rats prior to surgery, a whole-brain general linear modeling analysis was performed on averaged brain response to 1g and 3g air-puff stimuli. Unilateral stimulation on either the left (N = 19; Figure 2A, Table 1) or right (N = 20; Figure 2B, Table 2) paw resulted in significant activations in the bilateral primary sensory cortex hindlimb region (S1HL), thalamus (Tha), anterior cingulate cortex (ACC), insular cortex (Ins), secondary somatosensory cortex (SII), and caudate putamen (CPu) (voxel-wise cluster-forming threshold of $Z > 2.58$ and cluster significance threshold of $p < 0.05$). The signal time course from the peak activation in the contralateral S1HL during left paw stimulation indicated that fMRI signal strength increased during each epoch of air-puff and gradually returned to baseline after the end of stimulation.

Furthermore, the magnitude of the BOLD response was proportional to air-puff stimulus intensity. The pattern of signal time course was replicated in the contralateral S1HL corresponding to right paw stimulation (Figure 2C).

Encoding of Stimulus Intensity in S1HL

To identify all brain areas related to stimulation intensity encoding, we performed a whole-brain paired t-test analysis of the difference of brain activation between 1g and 3g stimuli to left paw stimulation in all rats prior to injury at baseline. The 3g stimulus evoked significantly stronger responses than 1g stimulus in the contralateral S1HL and caudal part of ACC (N = 19; Figure 3A, Table 3). No brain area exhibited stronger activity to 1g than 3g stimuli (paired-t test, with voxel-wise cluster-forming threshold of $Z > 2.58$ and cluster significance threshold of $p < 0.05$).

In the post-hoc analysis, we extracted BOLD response magnitude (β estimates) in S1HL derived from the peak of average innocuous air-puff stimulation to left paw in Figure 3A. We find that in SNI rats, the differential S1HL responses to the two air-puff stimuli of the left paw were essentially identical at baseline (N = 12) and at 5 (N = 10) and 28 days (N = 7) after SNI injury, despite one of the innocuous air-puffs being above SNI's tactile withdrawal threshold, at 28 days post-surgery. Overall, SNI and sham surgery rats exhibited similar S1HL responses (Figure 3B).

BOLD magnitude was significantly associated with stimulus intensity (three-way ANOVA, stimulus intensity effect $F(1, 90) = 20.24$, $p < 0.001$). Furthermore, the S1HL BOLD magnitude elicited by the 3g stimulus was consistent over time, as it was not significantly different at 28 days post-SNI compared to the baseline (three-way ANOVA, Fisher LSD post-hoc comparison, $p = 0.34$). Similarly, S1HL BOLD magnitude was not different between SNI and sham surgery groups 28 days post-surgery (Fisher LSD post-hoc comparison, $p = 0.42$). The magnitude of responses in S1HL were not significantly different among air-puff intensity over time (stimulus intensity-by-time effect $F(2, 90) = 1.25$, $p = 0.29$), and also were not significantly different among group over time (group-by-time effect $F(2, 90) = 1.07$, $p = 0.35$). These results demonstrate that activation in S1HL reflected stimuli intensity, and this was unchanged following neuropathic injury and the presence of tactile allodynia, as determined behaviorally.

Association of NAc and Prefrontal Areas with Tactile Allodynia

To identify brain activity specifically associated with tactile allodynia, a whole-brain paired t-test was used to identify different BOLD responses to stimulation of the SNI-injured paw, pre- and post-surgery. During 3g stimulation, no significant difference between baseline and 5 days post-SNI was observed (N = 10; data not shown, paired t-test, with voxel-wise cluster-forming threshold of $Z > 2.3$ and cluster significance threshold of $p < 0.05$). When pain became chronic at 28 days post-SNI surgery, 3g stimuli to the injured paw resulted in decreased signal compared to baseline in many brain regions, including ipsilateral NAc, contralateral OFC, mPFC, Ins, and bilateral CPu (N = 7; Figure 4, Table 4, paired t-test, with voxel-wise cluster-forming threshold of $Z > 2.3$ and cluster significance threshold of $p < 0.05$). No significant change was observed in the sham animals in both 5 (N = 9) and 28 (N=

6) days post-surgery, with 1g stimulus in all test conditions (data not shown, paired t-test, with voxel-wise cluster-forming threshold of $Z > 2.3$ and cluster significance threshold of $p < 0.05$).

In the post-hoc analysis, we extracted β estimates of BOLD response within these regions, as shown in Figure 4A. NAc and mPFC signals were significantly different over time within the injured group (three-way ANOVA, group-by-time effect $F(2, 90) = 3.22$, $p = 0.04$ for NAc and $F(2, 90) = 3.72$, $p = 0.03$ for mPFC), whereas OFC was significantly different for stimulus intensity over time (stimulus intensity-by-time effect $F(2, 90) = 4.67$, $p = 0.01$). Longitudinal signal changes of NAc and OFC are shown in Figure 4B and 4C. NAc exhibited a significant deactivation at 28 days post-SNI to 3g stimulus, but not to 1g stimulus (Figure 4B; Fisher LSD post-hoc comparison on difference between 1 and 3g stimulus at day 28, $p = 0.042$; difference of 3g stimulus response between baseline and day 28, $p < 0.001$). No significant signal change was seen in the sham rats to both stimuli (Figure 4B). BOLD signal in NAc displayed a positive response to 3g stimulus at baseline, whereas the identical stimulus evoked a trend of two peaks of deactivation at 28 days post SNI (Figure 4C), with the second peak of deactivation at 1 TR (2 second) after stimulus offset. OFC displayed a significant deactivation at 28 days post SNI to 3g stimulus, but not to 1g stimulus (Figure 4D; Fisher LSD post-hoc comparison on difference between 1g and 3g stimulus at day 28, $p < 0.033$; difference of 3g stimulus response between baseline and day 28, $p < 0.001$). While activation was observed in OFC during 3g stimulus at baseline, deactivation was seen at 28 days post SNI (Figure 4E).

Discussion

To identify brain changes associated with persistent tactile allodynia, this study used a longitudinal approach and evaluated differential brain responses to innocuous tactile stimuli between pre- and post-partial peripheral nerve injury (SNI model). Because pain perception and related behavior require a conscious and aroused state, and because anesthesia dampens BOLD activity, assessment of brain activity in awake animals was deemed critical for accurate identification of tactile allodynia-related brain activity. We therefore used protocols we have recently established for performing fMRI in the awake rat, with proper animal habituation and minimal restraint, permitting brain scans uncontaminated with anesthesia or excessive movement [16]. The main result of this study is that the primary somatosensory cortex likely encodes the intensity of tactile inputs, but does not discriminate nociceptive touch following neuropathic injury. Moreover, the abnormal brain responses observed for a normally innocuous stimulus at 28 days post-neuropathic injury suggests long-lasting brain changes in the NAc and prefrontal brain areas, demonstrating the importance of corticolimbic processing in chronic neuropathic pain.

In healthy rats prior to surgery, innocuous air-puff stimulation evoked responses within a large distributed array of subcortical and cortical brain areas, including bilateral somatosensory cortices, thalamus, insular cortex, and anterior cingulate cortex. This brain representation was consistent when the stimulation was presented to either paw. Our data show that in the healthy condition, S1 displays graded BOLD responses with the intensity of the tactile stimulus. While it is possible that this may indicate a general shift in attention due

to a startle response, this result is also consistent with the idea that neural activity in S1 has a principal role in innocuous cutaneous sensory-discriminative processing. According to the traditional view of pain, which posits that BOLD activity in SI encodes a discriminative component of pain [3; 14; 47] and the general hypothesis that tactile allodynia reflects low-threshold Aβ fibers gaining access to spinal nociceptive neurons, we expected S1 to exhibit a low response to innocuous stimuli and a larger response to similar stimuli during tactile allodynia. However, we found that the S1 response magnitude after nerve injury remained equivalent to that evoked by identical stimuli prior to the injury. This result implies that the presence or absence of nociceptive input is not a main determinant of S1 activation after neuropathic injury. This result is not as clear in current pain research in humans, where concurrent activation of S1 during acute pain is prevalent [3]. For example, a term based meta-analysis (www.neurosynth.org) identifies that the S1 leg/foot region in the right hemisphere exhibits a z-score of 8.0 for the reverse inference of the term “pain” (N = 420 studies, without correcting for variations of body site stimulated, and >90% of identified studies being done in healthy subjects for acute pain). Consistently, in a phase-encoded human fMRI experiment, the nociceptive S1 map was found to be precisely aligned with tactile maps obtained by innocuous somatosensory stimuli of the hand [34]. Our experiment, on the other hand, differs from these in that our allodynia paradigm was designed to dissociate stimulus magnitude from pain. In this way, the activity we observed in S1 is consistent with the idea that S1 encodes stimulus magnitude separately from pain. This parralels a recent study showing S1 diminished pain-related activity following the transition to a chronic pain state [22], and is in line with the observation that nociceptive input to S1 is sparse, as there have been no cortical columns found to be nociceptive-specific [25; 26].

The present behavioral results show that tactile allodynia is clearly present 5 days after neuropathic injury, yet related brain activity was only detected 28 days after injury and localized primarily in the prefrontal (mPFC, OFC), striatum (especially NAc) and SII/Insula areas. In two previous studies, we have reported resting state functional connectivity changes in a similar longitudinal study after SNI injury in rats under anesthesia [6; 15]. There is temporal consistency across all three studies, as they all show that tactile allodynia, as well as whole-brain functional connectivity, NAc functional connectivity, and decreases in gene expression levels of NAc dopamine 1A, 2, and kappa-opioid were all observable in the brain only 28 days after neuropthic injury. Together these results suggest that macroscopic brain reorganization is a consequence of pain behavior established weeks prior. However, cellular changes are observable far earlier, with upregulated gene expression covariance, and robust changes in electrophysiology and cell morphology in the nucleus accumbens [41; 43] occuring as soon as 5 days after SNI. Thus, corticolimbic brain circuitry seems to undergo large changes at the cellular level within days after induction of SNI, yet the imprint of these changes may not be large enough to be observed in fMRI scans and requires further elaboration until it becomes evident at about 1 month after SNI injury.

The brain areas linked with tactile allodynia in the current study are critical components of mesolimbic circuitry. The mPFC, for example, has been heavily implicated in the formation of subjective pain perception and experience related to incoming sensory stimuli [4; 7; 18; 27]. Marked morphological and functional changes of neurons in mPFC are found in rats with neuropathic pain [35]; and optogenetic stimulation of mPFC relieves tactile allodynia

of neuropathic pain [29], as well as anxiety-like behaviours in mice with chronic inflammatory pain [51]. Moreover, the increased excitability of mPFC decreases reward-seeking behavior and interferes with striatal dopamine signaling [20]. Although our contrast maps generally indicate an overall decreased BOLD signal in the areas associated with tactile allodynia, the temporal patterns of BOLD within both NAc and OFC are similar to those reported in chronic pain patients during acute painful stimulation [8; 11], especially for the NAc, which also correlated to shifts in emotional valuation for thermal painful stimuli in relation to the patients' ongoing back pain [8]. In addition, in our own literature search on tactile allodynia, 9 out of 15 neuroimaging studies reported marked changes of activity in the prefrontal cortex. Taken together with the present study and the accumulating evidence that shows a critical role of mesocorticolimbic circuitry in pain chronification [5], we conclude that a shift in emotional valuation and motivation circuitry, rather than sensory encoding circuitry, underlies tactile allodynia.

While our results show that abnormal activity in prefrontal areas and NAc is a marker of allodynia, caution should be made when interpreting the negative BOLD signal. The existence of the negative fMRI BOLD response has been studied for quite some time [1; 48]; yet, to date, its origins remain elusive. Numerous hypotheses have been proposed to account for its occurrence [28; 31; 36; 45; 50]. In conditions when inhibitory circuits are involved, the negative BOLD response could be due to the impact of inhibitory postsynaptic potentials (IPSPs) on blood flow; as a result, BOLD activity may be reduced below the baseline level in response to particular stimuli. However, it is also possible that brain areas showing a negative BOLD response actually have an *increased* neuronal activity during the stimulation, but for some reason these brain areas do not receive a corresponding increase in their blood oxygenation. It is not know whether negative BOLD response is simply the inverted neurophysiological fingerprint of the positive response [37]. This having been said, and despite the inherent limitations of fMRI, this study highlights the brain regions of SNI rats where there is an abnormal response to a normally innocuous stimulus. This is a critical step towards understanding the brain mechanisms of tactile allodynia. The precise characteristics of how mesocorticolimbic reorganization is involved in tactile allodyia remain to be uncovered.

Finally, brain data from conscious animals is key to establishing a useful translational link to human brain function, especially in pain processing where consciousness is necessary for the pain experience. There are many challenges in collecting such data, such as excessive movement during scans, and the stress induced during acclimation, which can induce unintended physiological effects [32]. However, we have recently shown that, with proper intstrumental setup and acclimation to the scanning environment [16], animals can remain conscious, still, and feel comfortable during fMRI under minimal stress, entirely without the use of anesthesia. This data is critical to pain research, and we urge others to further improve upon current methods so that the most accurate assessment of conscious pain processing can be captured in the animal brain.

To summarize, this study demonstrates that the BOLD response in S1 encodes somatosensory stimulus intensity, and does not display a specific dependence upon nociception following a neuropathic injury. Additionally, we show that the presence of

tactile allodynia in persistent neuropathic pain may be associated with a shift of brain responses towards neural circuits that regulate the affective and motivational components of pain.

Acknowledgments

This work was supported by the National Institute of Health Blueprint grant NIDCR DE022746. We thank Apkarian lab members for reading and providing comments on earlier versions of this manuscript. We also thank Dr. Baliki for advising on fMRI analysis methods.

References

1. Allison JD, Meador KJ, Loring DW, Figueroa RE, Wright JC. Functional MRI cerebral activation and deactivation during finger movement. Neurology. 2000; 54(1):135–142. [PubMed: 10636139]
2. Apkarian AV, Baliki MN, Geha PY. Towards a theory of chronic pain. Progress in neurobiology. 2009; 87(2):81–97. [PubMed: 18952143]
3. Apkarian AV, Bushnell MC, Treede RD, Zubieta JK. Human brain mechanisms of pain perception and regulation in health and disease. European journal of pain. 2005; 9(4):463–484. [PubMed: 15979027]
4. Apkarian AV, Sosa Y, Sonty S, Levy RM, Harden RN, Parrish TB, Gitelman DR. Chronic back pain is associated with decreased prefrontal and thalamic gray matter density. The Journal of neuroscience : the official journal of the Society for Neuroscience. 2004; 24(46):10410–10415. [PubMed: 15548656]
5. Baliki MN, Apkarian AV. Nociception, Pain, Negative Moods, and Behavior Selection. Neuron. 2015; 87(3):474–491. [PubMed: 26247858]
6. Baliki MN, Chang PC, Baria AT, Centeno MV, Apkarian AV. Resting-sate functional reorganization of the rat limbic system following neuropathic injury. Scientific reports. 2014; 4:6186. [PubMed: 25178478]
7. Baliki MN, Geha PY, Apkarian AV. Parsing pain perception between nociceptive representation and magnitude estimation. Journal of neurophysiology. 2009; 101(2):875–887. [PubMed: 19073802]
8. Baliki MN, Geha PY, Fields HL, Apkarian AV. Predicting value of pain and analgesia: nucleus accumbens response to noxious stimuli changes in the presence of chronic pain. Neuron. 2010; 66(1):149–160. [PubMed: 20399736]
9. Baliki MN, Schnitzer TJ, Bauer WR, Apkarian AV. Brain morphological signatures for chronic pain. PloS one. 2011; 6(10):e26010. [PubMed: 22022493]
10. Baron R. Mechanisms of disease: neuropathic pain--a clinical perspective. Nature clinical practice Neurology. 2006; 2(2):95–106.
11. Becerra L, Borsook D. Signal valence in the nucleus accumbens to pain onset and offset. European journal of pain. 2008; 12(7):866–869. [PubMed: 18226937]
12. Becerra L, Morris S, Bazes S, Gostic R, Sherman S, Gostic J, Pendse G, Moulton E, Scrivani S, Keith D, Chizh B, Borsook D. Trigeminal neuropathic pain alters responses in CNS circuits to mechanical (brush) and thermal (cold and heat) stimuli. The Journal of neuroscience : the official journal of the Society for Neuroscience. 2006; 26(42):10646–10657. [PubMed: 17050704]
13. Bridges D, Thompson SW, Rice AS. Mechanisms of neuropathic pain. Br J Anaesth. 2001; 87(1): 12–26. [PubMed: 11460801]
14. Bushnell MC, Duncan GH, Hofbauer RK, Ha B, Chen JI, Carrier B. Pain perception: is there a role for primary somatosensory cortex? Proc Natl Acad Sci U S A. 1999; 96(14):7705–7709. [PubMed: 10393884]
15. Chang PC, Pollema-Mays SL, Centeno MV, Procissi D, Contini M, Baria AT, Martina M, Apkarian AV. Role of nucleus accumbens in neuropathic pain: linked multi-scale evidence in the rat transitioning to neuropathic pain. Pain. 2014; 155(6):1128–1139. [PubMed: 24607959]

16. Chang PC, Procissi D, Bao Q, Centeno MV, Baria A, Apkarian AV. Novel method for functional brain imaging in awake minimally restrained rats. Journal of neurophysiology. 2016 jn 01078 02015.
17. Chaplan SR, Bach FW, Pogrel JW, Chung JM, Yaksh TL. Quantitative assessment of tactile allodynia in the rat paw. Journal of neuroscience methods. 1994; 53(1):55–63. [PubMed: 7990513]
18. Coghill RC, Sang CN, Maisog JM, Iadarola MJ. Pain intensity processing within the human brain: a bilateral, distributed mechanism. Journal of neurophysiology. 1999; 82(4):1934–1943. [PubMed: 10515983]
19. Costigan M, Scholz J, Woolf CJ. Neuropathic pain: a maladaptive response of the nervous system to damage. Annual review of neuroscience. 2009; 32:1–32.
20. Ferenczi EA, Zalocusky KA, Liston C, Grosenick L, Warden MR, Amatya D, Katovich K, Mehta H, Patenaude B, Ramakrishnan C, Kalanithi P, Etkin A, Knutson B, Glover GH, Deisseroth K. NEURAL CIRCUITS Prefrontal cortical regulation of brainwide circuit dynamics and reward-related behavior. Science. 2016; 351(6268):41–U59.
21. Geha PY, Baliki MN, Wang X, Harden RN, Paice JA, Apkarian AV. Brain dynamics for perception of tactile allodynia (touch-induced pain) in postherpetic neuralgia. Pain. 2008; 138(3):641–656. [PubMed: 18384958]
22. Hashmi JA, Baliki MN, Huang L, Baria AT, Torbey S, Hermann KM, Schnitzer TJ, Apkarian AV. Shape shifting pain: chronification of back pain shifts brain representation from nociceptive to emotional circuits. Brain. 2013; 136(Pt 9):2751–2768. [PubMed: 23983029]
23. Hofbauer RK, Olausson HW, Bushnell MC. Thermal and tactile sensory deficits and allodynia in a nerve-injured patient: a multimodal psychophysical and functional magnetic resonance imaging study. The Clinical journal of pain. 2006; 22(1):104–108. [PubMed: 16340599]
24. Jensen TS, Finnerup NB. Allodynia and hyperalgesia in neuropathic pain: clinical manifestations and mechanisms. The Lancet Neurology. 2014; 13(9):924–935. [PubMed: 25142459]
25. Kenshalo DR, Iwata K, Sholas M, Thomas DA. Response properties and organization of nociceptive neurons in area 1 of monkey primary somatosensory cortex. Journal of neurophysiology. 2000; 84(2):719–729. [PubMed: 10938299]
26. Kenshalo DR Jr, Chudler EH, Anton F, Dubner R. SI nociceptive neurons participate in the encoding process by which monkeys perceive the intensity of noxious thermal stimulation. Brain research. 1988; 454(1–2):378–382. [PubMed: 3409021]
27. Kong J, White NS, Kwong KK, Vangel MG, Rosman IS, Gracely RH, Gollub RL. Using fMRI to dissociate sensory encoding from cognitive evaluation of heat pain intensity. Human brain mapping. 2006; 27(9):715–721. [PubMed: 16342273]
28. Lauritzen M. Reading vascular changes in brain imaging: is dendritic calcium the key? Nature reviews Neuroscience. 2005; 6(1):77–85. [PubMed: 15611729]
29. Lee M, Manders TR, Eberle SE, Su C, D'Amour J, Yang R, Lin HY, Deisseroth K, Froemke RC, Wang J. Activation of corticostriatal circuitry relieves chronic neuropathic pain. The Journal of neuroscience : the official journal of the Society for Neuroscience. 2015; 35(13):5247–5259. [PubMed: 25834050]
30. Liljencrantz J, Bjornsdotter M, Morrison I, Bergstrand S, Ceko M, Seminowicz DA, Cole J, Bushnell MC, Olausson H. Altered C-tactile processing in human dynamic tactile allodynia. Pain. 2013; 154(2):227–234. [PubMed: 23290550]
31. Logothetis NK. What we can do and what we cannot do with fMRI. Nature. 2008; 453(7197):869–878. [PubMed: 18548064]
32. Low LA, Bauer LC, Pitcher MH, Bushnell MC. Restraint training for awake functional brain scanning of rodents can cause long-lasting changes in pain and stress responses. Pain. 2016; 157(8):1761–1772. [PubMed: 27058679]
33. Maihofner C, Schmelz M, Forster C, Neundorfer B, Handwerker HO. Neural activation during experimental allodynia: a functional magnetic resonance imaging study. The European journal of neuroscience. 2004; 19(12):3211–3218. [PubMed: 15217377]
34. Mancini F, Haggard P, Iannetti GD, Longo MR, Sereno MI. Fine-grained nociceptive maps in primary somatosensory cortex. The Journal of neuroscience : the official journal of the Society for Neuroscience. 2012; 32(48):17155–17162. [PubMed: 23197708]

35. Metz AE, Yau HJ, Centeno MV, Apkarian AV, Martina M. Morphological and functional reorganization of rat medial prefrontal cortex in neuropathic pain. Proc Natl Acad Sci U S A. 2009; 106(7):2423–2428. [PubMed: 19171885]
36. Moraschi M, DiNuzzo M, Giove F. On the origin of sustained negative BOLD response. Journal of neurophysiology. 2012; 108(9):2339–2342. [PubMed: 22723671]
37. Mullinger KJ, Mayhew SD, Bagshaw AP, Bowtell R, Francis ST. Evidence that the negative BOLD response is neuronal in origin: a simultaneous EEG-BOLD-CBF study in humans. Neuroimage. 2014; 94:263–274. [PubMed: 24632092]
38. Peeters RR, Tindemans I, De Schutter E, Van der Linden A. Comparing BOLD fMRI signal changes in the awake and anesthetized rat during electrical forepaw stimulation. Magnetic resonance imaging. 2001; 19(6):821–826. [PubMed: 11551722]
39. Petrovic P, Ingvar M, Stone-Elander S, Petersson KM, Hansson P. A PET activation study of dynamic mechanical allodynia in patients with mononeuropathy. Pain. 1999; 83(3):459–470. [PubMed: 10568854]
40. Pisauro MA, Dhruv NT, Carandini M, Benucci A. Fast hemodynamic responses in the visual cortex of the awake mouse. The Journal of neuroscience : the official journal of the Society for Neuroscience. 2013; 33(46):18343–18351. [PubMed: 24227743]
41. Ren W, Centeno MV, Berger S, Wu Y, Na X, Liu X, Kondapalli J, Apkarian AV, Martina M, Surmeier DJ. The indirect pathway of the nucleus accumbens shell amplifies neuropathic pain. Nature neuroscience. 2016; 19(2):220–222. [PubMed: 26691834]
42. Sandkuhler J. Models and mechanisms of hyperalgesia and allodynia. Physiological reviews. 2009; 89(2):707–758. [PubMed: 19342617]
43. Schwartz N, Temkin P, Jurado S, Lim BK, Heifets BD, Polepalli JS, Malenka RC. Chronic pain. Decreased motivation during chronic pain requires long-term depression in the nucleus accumbens. Science. 2014; 345(6196):535–542. [PubMed: 25082697]
44. Schwarz AJ, Danckaert A, Reese T, Gozzi A, Paxinos G, Watson C, Merlo-Pich EV, Bifone A. A stereotaxic MRI template set for the rat brain with tissue class distribution maps and co-registered anatomical atlas: application to pharmacological MRI. Neuroimage. 2006; 32(2):538–550. [PubMed: 16784876]
45. Shmuel A, Augath M, Oeltermann A, Logothetis NK. Negative functional MRI response correlates with decreases in neuronal activity in monkey visual area V1. Nature neuroscience. 2006; 9(4): 569–577. [PubMed: 16547508]
46. Silva AC, Koretsky AP, Duyn JH. Functional MRI impulse response for BOLD and CBV contrast in rat somatosensory cortex. Magnetic resonance in medicine : official journal of the Society of Magnetic Resonance in Medicine / Society of Magnetic Resonance in Medicine. 2007; 57(6): 1110–1118.
47. Timmermann L, Ploner M, Haucke K, Schmitz F, Baltissen R, Schnitzler A. Differential coding of pain intensity in the human primary and secondary somatosensory cortex. Journal of neurophysiology. 2001; 86(3):1499–1503. [PubMed: 11535693]
48. Tootell RB, Hadjikhani N, Hall EK, Marrett S, Vanduffel W, Vaughan JT, Dale AM. The retinotopy of visual spatial attention. Neuron. 1998; 21(6):1409–1422. [PubMed: 9883733]
49. van Hecke O, Austin SK, Khan RA, Smith BH, Torrance N. Neuropathic pain in the general population: a systematic review of epidemiological studies. Pain. 2014; 155(4):654–662. [PubMed: 24291734]
50. Wade AR. The negative BOLD signal unmasked. Neuron. 2002; 36(6):993–995. [PubMed: 12495615]
51. Wang GQ, Cen C, Li C, Cao S, Wang N, Zhou Z, Liu XM, Xu Y, Tian NX, Zhang Y, Wang J, Wang LP, Wang Y. Deactivation of excitatory neurons in the prelimbic cortex via Cdk5 promotes pain sensation and anxiety. Nature communications. 2015; 6:7660.

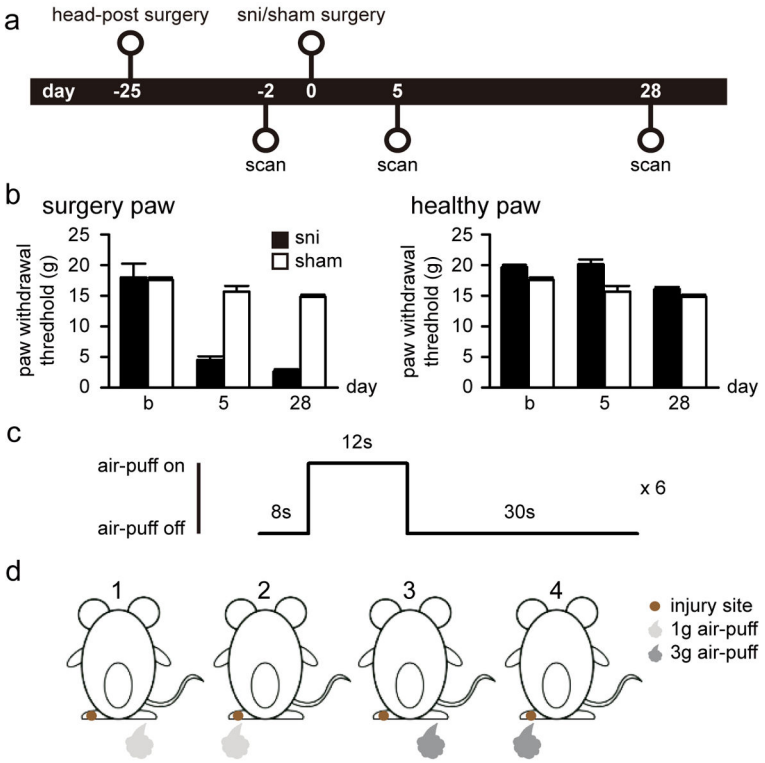

Figure 1. Experimental design

(a) Twenty-two rats were included in the study and imaged 2 days before the surgery as baseline. Rats were then randomized and underwent peripheral neuropathic (SNI, N = 12) and sham (N = 10) surgeries, and imaged again at 5 and 28 days post surgery. Tests for paw withdrawal threshold were performed the day before each scan. **(b)** SNI rats displayed tactile allodynia for stimuli applied to the neuropathic injured paw, at 5 and 28 days after surgery. No significant change in paw withdrawal threshold was observed in the healthy paw in either SNI or sham rats. **(c)** fMRI scan with periodic air-puff stimulation had 6 repetitive stimulus blocks. Each block consisted of stimulation alternated with 8sec-off/12sec-on/30sec-off. **(d)** fMRI scans were conducted when rats received 1g or 3g air-puffs to left (injury site) or right (healthy) paw. The 4th condition was expected to produce allodynia behavior after SNI surgery.

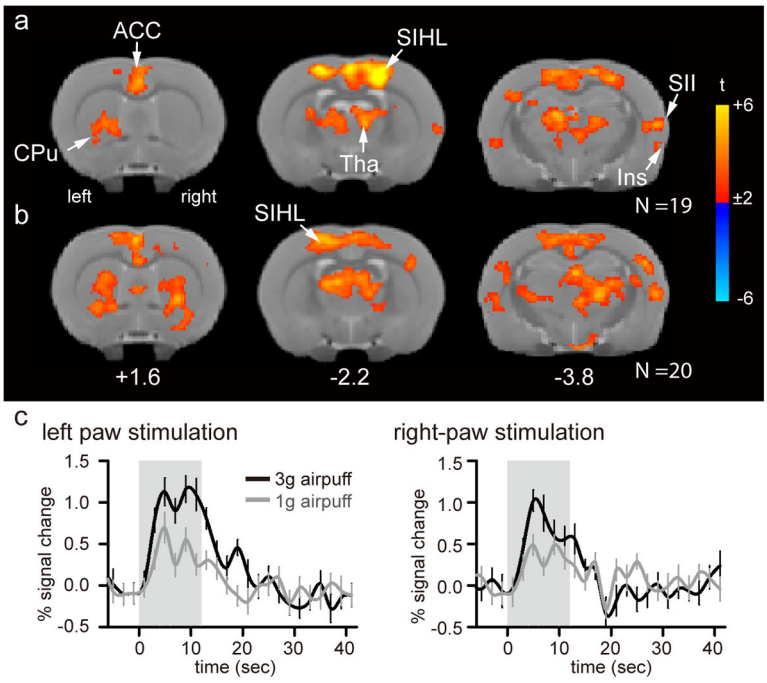

Figure 2. Brain representation of tactile stimulation in healthy rats prior to injury

(a, b) Group average maps in response to unilateral left (a) and right (b) paw stimulation (one-sample t-test, with voxel-wise cluster threshold of $Z > 2.58$ and cluster significance threshold of $p < 0.05$; $N = 19$ for left paw, $N = 20$ for right paw, corrected for multiple comparisons). Group-averaged maps are displayed as statistical t-values overlaid on corresponding T2-weighted anatomical images. Color bars represent the range of t-values. The distance from the Bregma in mm is shown at the bottom. **(c)** Percent signal changes over time in the corresponding contralateral SIHL are shown. Abbreviation: SIHL – primary sensory cortex hind limb region, SII – secondary sensory cortex, Tha – thalamus, ACC – anterior cingulate cortex, Ins – insular cortex, and CPu – caudate putamen.

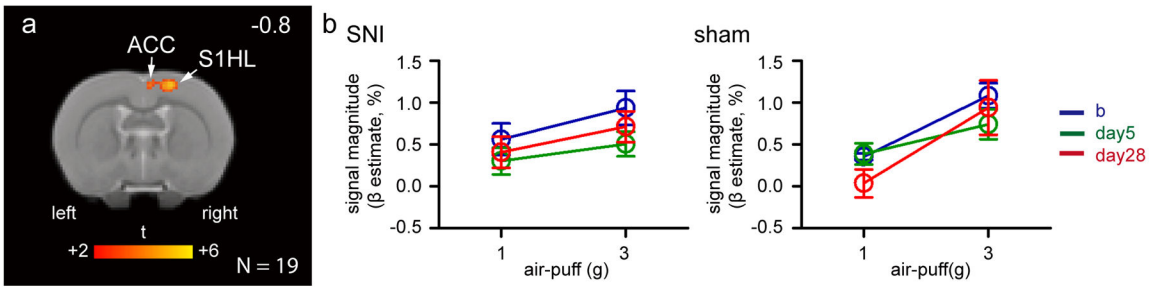

Figure 3. Activity in somatosensory cortex (SIHL) reflects stimulus intensity independently of neuropathic injury

(a) Brain areas exhibiting stronger response to 3g than 1g air-puffs applied to the left hind paw at baseline (paired-t test, with voxel-wise cluster threshold of $Z > 2.58$ and cluster significance threshold of $p < 0.05$ corrected for multiple comparisons; $N = 19$). Only contralateral S1HL and ACC encode stimulus intensity at baseline. The distance from the Bregma in mm is shown at the top right. Abbreviations same as in figure 2. **(b)** Magnitude of the BOLD signal in the contralateral SIHL to left paw stimulation in SNI and sham rats display increased activity with increased stimulus intensity, despite one of the air-puffs being above SNI's paw withdrawal threshold at day 28 post-surgery. Abbreviation: b – baseline, day5 – 5 days post-surgery, day28 – 28 days post-surgery, and also refer to abbreviations in Figure 2.

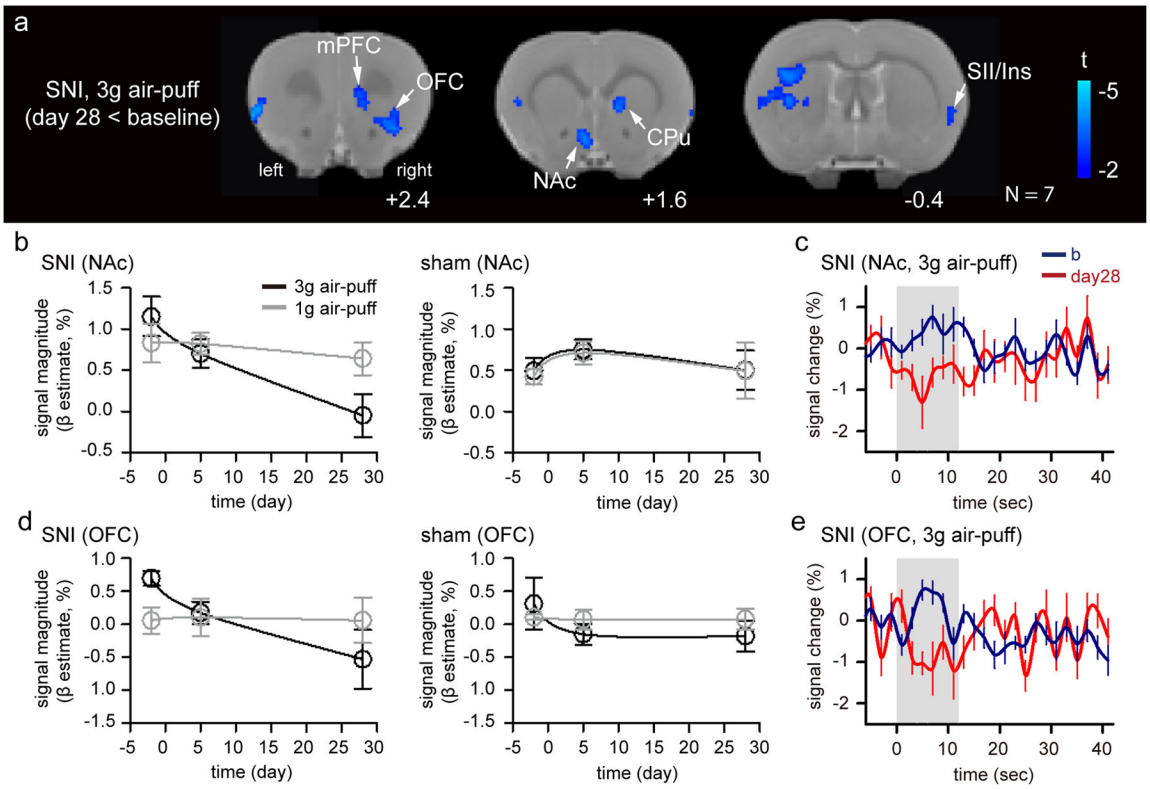

Figure 4. Brain activity associated with tactile allodynia

(a) Group difference in brain activity between day 28 and baseline in response to 3g air-puff stimulation on the injured paw in the SNI rats (paired t-test, with voxel-wise cluster-forming threshold of $Z > 2.3$ and cluster significance threshold of $p < 0.05$ corrected for multiple comparisons; N =7). **(b)** BOLD magnitude of NAc in SNI and sham rats is significantly different between the groups over time. **(c)** BOLD signal of NAc in SNI rats to the identical stimulation at baseline and 28 days post-surgery. **(d)** BOLD magnitude of OFC in SNI and sham rats is significantly different between the groups over time. **(e)** BOLD signal changes in OFC of SNI rats to the identical stimulation at baseline and 28 days post-surgery. Abbreviation: mPFC – medial frontal cortex, OFC – orbital frontal cortex, NAc – nucleus accumbens, b – baseline, day28 – 28 days post-surgery and also refer to abbreviations in Figure 2.

Table 1

Brain activity for left paw air-puff stimulation in healthy rats, prior to peripheral injury

				Coordinate		
Volume	**Anatomical Structure**		**t-value**	**x**	**y**	**z**
Activation						
9729	R	primary somatosensory cortex, hindlimb region	8.3	21.3	−13.6	−10.0
	L	primary somatosensory cortex, hindlimb region	6.3	−21.3	−13.6	−12.0
	R	primary somatosensory cortex, trunk region	6.1	27.1	−13.6	−24.0
	R	anterior cingulate cortex	6.6	0.0	−25.2	24.0
	R	secondary motor cortex	6.2	5.8	−11.6	−8.0
	R	anterodorsal thalamic nucleus	4.5	11.6	−42.7	−16.0
325	R	secondary somatosensory cortex	5.8	64.0	−52.3	−22.0
			3.6	58.2	−48.5	−26.0
	R	dysgranular insular cortex	3.3	64.0	−62.0	−28.0
254	R	lateral stripe of the striatum	4.3	31.0	−69.8	16.0
	R	ventral orbital cortex	4.4	34.9	−62.0	22.0
	R	caudate putamen	3.5	23.3	−58.2	14.0
228	L	secondary auditory cortex, ventral area	4.0	−62.0	−54.3	−40.0
	L	ectorhinal cortex	4.1	−58.2	−62.0	−32.0
	L	secondary somatosensory cortex	3.5	−58.2	−50.4	−20.0
	L	dysgranular insular cortex	3.4	−52.3	−60.1	−26.0
	L	agranular insular cortex, posterior part	3.2	−56.2	−67.9	−24.0

List of activated brain regions. One-sample t-test, with voxel-wise cluster-forming threshold of $Z > 2.58$ and cluster significance threshold of $p < 0.05$, corrected for multiple comparisons. Volumes are expressed in number of voxels. Coordinates (mm) are in standard space. Abbreviations: R = right, L = left of the brain.

Table 2

Brain activity for right paw air-puff stimulation in healthy rats prior to peripheral injury

				Coordinate		
Volume	**Anatomical Structure**		**t-value**	**x**	**y**	**z**
Activation						
10958	R	secondary motor cortex	5.9	0.0	−7.8	−8.0
	L	anteroventral thalamic nucleus, dorsomedial part	6.4	−15.5	−44.6	−20.0
	R	anteroventral thalamic nucleus, dorsomedial part	6.0	17.4	−48.5	−22.0
	R	retrosplenial agranular cortex	6.3	5.8	−9.7	−44.0
	L	primary somatosensory cortex, hindlimb region	6.0	−17.4	−13.6	−10.0
	R	posterior thalamic nuclear group	5.7	19.4	−52.3	−32.0
1478	R	secondary auditory cortex, ventral area	4.9	62.0	−52.3	−34.0
	R	primary somatosensory cortex, barrel field	4.8	52.3	−27.1	−38.0
			4.8	52.3	−27.1	−46.0
			4.7	54.3	−29.1	−26.0
	R	secondary auditory cortex, ventral area	4.0	65.9	−54.3	−42.0
	R	secondary somatosensory cortex	4.0	64.0	−50.4	−26.0
1183	R	caudate putamen	4.3	27.1	−58.2	6.0
			3.5	34.9	−65.9	2.0
			3.5	25.2	−44.6	0.0
	R	olfactory tubercle	4.7	19.4	−79.5	18.0
			3.9	3.9	−71.7	28.0
	R	dorsal endopiriform nucleus	3.7	34.9	−65.9	16.0
717	L	secondary auditory cortex, dorsal area	3.8	−56.2	−36.8	−44.0
	L	secondary auditory cortex, ventral area	3.8	−52.3	−56.2	−34.0
			3.6	−64.0	−52.3	−42.0
	L	caudate putamen	4.4	−50.4	−64.0	−20.0
	L	primary auditory cortex	3.9	−62.0	−31.0	−46.0
			4.3	−64.0	−44.6	−40.0
475	R	tuber cinereum area	4.2	11.6	−89.2	−36.0
	R	lateral hypothalamic area	4.2	13.6	−87.2	−44.0

Volume	Anatomical Structure		t-value	Coordinate		
				x	y	z
	L	lateral hypothalamic area	3.8	−13.6	−79.5	−42.0
	R	ventromedial hypothalamic nucleus, ventrolateral part	3.9	7.8	−93.1	−30.0
	L	hypothalamus, ventral intermediate tissue	3.7	−9.7	−93.1	−40.0
	R	hypothalamus, dorsal intermediate tissue	3.5	15.5	−67.9	−42.0
267	L	ventral posteromedial thalamic nucleus	3.7	−25.2	−52.3	−40.0
	L	laterodorsal thalamic nucleus, dorsomedial part	3.3	−29.1	−42.7	−40.0
	L	zona incerta, ventral part	3.3	−31.0	−58.2	−46.0
	L	ventral lateral geniculate nucleus, magnocellular part	2.9	−40.7	−52.3	−46.0

List of activated brain regions. One-sample t-test, with voxel-wise cluster-forming threshold of $Z > 2.58$ and cluster significance threshold of $p < 0.05$, corrected for multiple comparisons. Volumes are expressed in number of voxels. Coordinates (mm) are in standard space. Abbreviations: R = right, L = left of the brain.

Table 3

Brain areas with graded responses to the left paw stimulation in healthy rats prior to peripheral injury

				Coordinate		
Volume	**Anatomical Structure**		**t-value**	**x**	**y**	**z**
3g > 1g stimulation						
278	R	primary somatosensory cortex, hindlimb region	4.4	*17.4*	*−9.7*	*−12.0*
			3.4	25.2	−13.6	−16.0
	R	anterior cingulate cortex	4.4	9.7	−9.7	−16.0

List of activated brain regions. Paired-t test, with voxel-wise cluster-forming threshold of Z > 2.58 and cluster significance threshold of p < 0.05, corrected for multiple comparisons. Volumes are expressed in number of voxels. Coordinates (mm) are in standard space. Abbreviations: R = right, L = left of the brain.

Table 4

Group difference between day 28 and baseline in response to 3g air-puff stimulation applied to the injured paw in SNI rats

				Coordinate		
Volume	**Anatomical Structure**		**t-value**	**x**	**y**	**z**
Baseline > 28 days post-SNI						
846	L	granular insular cortex	−3.9	−52.3	−52.3	24.0
	L	primary somatosensory cortex, upper lip region	−4.0	−48.5	−42.7	4.0
	L	accumbens nucleus, shell	−3.9	−5.8	−67.9	18.0
	L	caudate putamen	−3.7	−38.8	−36.8	0.0
			−3.6	−27.1	−33.0	4.0
			−3.4	−40.7	−50.4	−4.0
256	R	ventral orbital cortex	−3.8	31.0	−60.1	26.0
	R	caudate putamen	−3.4	15.5	−48.5	18.0
			−3.1	13.6	−38.8	12.0
	R	prelimbic cortex	−3.0	11.6	−40.7	24.0
	R	agranular insular cortex, ventral part	−2.8	33.0	−50.4	24.0
	R	piriform layer	−2.7	34.9	−65.9	22.0
242	R	primary somatosensory cortex, upper lip region	−3.7	52.3	−48.5	4.0
	R	granular insular cortex	−3.5	58.2	−52.3	12.0
			−3.5	58.2	−56.2	0.0
	R	agranular insular cortex, posterior part	−2.9	58.2	−69.8	0.0

List of activated brain regions. Paired t-test, with voxel-wise cluster-forming threshold of $Z > 2.3$ and cluster significance threshold of $p < 0.05$, corrected for multiple comparisons. Volumes are expressed in number of voxels. Coordinates (mm) are in standard space. Abbreviations: R = right, L = left of the brain.